

Dynamic Self-Assembly Induced Rapid Dissolution of Cellulose at Low Temperatures

Jie Cai,[†] Lina Zhang,^{*,†} Shilin Liu,[†] Yating Liu,[†] Xiaojuan Xu,[†] Xuming Chen,[‡] Benjamin Chu,[‡] Xinglin Guo,[§] Jian Xu,[§] He Cheng,[§] Charles C. Han,[§] and Shigenori Kuga^{||}

Department of Chemistry, Wuhan University, Wuhan 430072, China; Department of Chemistry, Stony Brook University, Stony Brook, New York 11794-3400; State Key Laboratory of Polymer Physics and Chemistry, Institute of Chemistry, Chinese Academy of Sciences, Beijing 100080, China; and Graduate School of Agricultural and Life Sciences, The University of Tokyo, Tokyo, Japan

Received May 18, 2008; Revised Manuscript Received September 18, 2008

ABSTRACT: Cellulose can be dissolved in precooled ($-12\text{ }^{\circ}\text{C}$) 7 wt % NaOH–12 wt % urea aqueous solution within 2 min. This interesting process, to our knowledge, represents the most rapid dissolution of native cellulose. The results from ^{13}C NMR, ^{15}N NMR, ^1H NMR, FT-IR, small-angle neutron scattering (SANS), transmission electron microscopy (TEM), and wide-angle X-ray diffraction (WAXD) suggested that NaOH “hydrates” could be more easily attracted to cellulose chains through the formation of new hydrogen-bonded networks at low temperatures, while the urea hydrates could not be associated directly with cellulose. However, the urea hydrates could possibly be self-assembled at the surface of the NaOH hydrogen-bonded cellulose to form an inclusion complex (IC), leading to the dissolution of cellulose. Scattering experiments, including dynamic and static light scattering, indicated that most cellulose molecules, with limited amounts of aggregation, could exist as extended rigid chains in dilute solution. Further, the cellulose solution was relatively unstable and could be very sensitive to temperature, polymer concentration, and storage time, leading to additional aggregations. TEM images and WAXD provided experimental evidence on the formation of a wormlike cellulose IC being surrounded with urea. Therefore, we propose that the cellulose dissolution at $-12\text{ }^{\circ}\text{C}$ could arise as a result of a fast dynamic self-assembly process among solvent small molecules (NaOH, urea, and water) and the cellulose macromolecules.

Introduction

Numerous new functional materials of cellulose are being developing over a broad range of applications because of the increasing demand for environmentally friendly and biocompatible products.¹ However, the stiff cellulose molecular chain and close chain packing through numerous hydrogen bonds in cellulose have made the dissolution of cellulose to be a difficult process in most common solvents. Thus, solvent systems, such as LiCl–*N,N*-dimethylacetamide (DMAc), *N*-methylmorpholine *N*-oxide (NMMO), and ionic liquids, were developed to dissolve cellulose mostly at elevated temperatures.^{2–4} Recently, we have developed a novel solvent for the fast dissolution of cellulose by quickly stirring cellulose in a precooled ($-12\text{ }^{\circ}\text{C}$) 7 wt % NaOH–12 wt % urea aqueous solution.^{5,6} The native cellulose could be dissolved rapidly (within 2 min) in the novel solvent system to prepare a fairly transparent solution, indicating the absence of microphase separation. Moreover, a series of studies have been reported in our laboratory to indicate (1) the solvent can dissolve cellulose to prepare dilute and concentrated cellulose solutions,^{5,7} (2) the cellulose solution is very sensitive to temperature and polymer concentration,⁶ (3) novel cellulose fibers and functional materials have been spun successfully from the cellulose dope,^{8–10} and (4) derivatives of cellulose have been homogeneously synthesized in aqueous solution.¹¹ The rapid dissolution of cellulose at low temperatures is an exciting and surprising phenomenon. A worthwhile endeavor would be to first clarify why cellulose could be dissolved at low temperatures, instead of promoting dissolution by the normal heating pathway, and why the dissolution rate is so very fast.

It is well-known that dissolution of normal polymers includes a slow diffusion based on the interchangeability of solvent and polymer and needs a long time (the heating may accelerate the process). Obviously, our finding differs from the traditional dissolution process. It is worth noting that liquid water forms clusters via a dynamic supramolecular assembly process mainly through hydrogen bonds. The proportion of “network water” increases steadily as the temperature is lowered.¹² It is not hard to imagine that the promotion on a dissolution process by cooling may be related to the formation of hydrogen-bonded networks between cellulose and solvent components. A self-assembly acts as a pathway for the autonomous organization of components.¹³ There are two main kinds of self-assembly process: static, which is stable, and dynamic. For front, macromolecules can lead toward ordered various aggregates, such as the multiwalled tubes,¹⁴ the giant polymer vesicles,¹⁵ the multicomponent structures of carbon nanotubes,¹⁶ the reverse polymeric micelles,¹⁷ and stable surfactant-free colloidal nanoparticles.¹⁸ The study of dynamic self-assembly processes is in its infancy¹³ and deals with steady-state structures maintained by a constant supply of energy¹⁹ and with complex spatial structures.²⁰ Tsunashima et al. have reported that in cellulose diacetate solution dissolved in DMAc below $-12\text{ }^{\circ}\text{C}$ the dynamical self-assemblies arise as dynamical fluctuations.²¹ The aim of the present work is to investigate the rapid dissolution of cellulose, as induced by a dynamical self-assembly process for the NaOH, urea, and cellulose components in water at low temperatures. The physical methods, including ^{13}C NMR, ^{15}N NMR, ^1H NMR, FT-IR, wide-angle X-ray diffraction, and small-angle neutron scattering, were used to provide experimental evidence on how the relatively complex solvent system can be used to dissolve cellulose at low temperatures. Transmission electron microscopy as well as dynamic and static light scattering were employed to provide a form of “direct visualiza-

* To whom correspondence should be addressed; e-mail lnzhang@public.wh.hb.cn; Tel +86-27-87219274; Fax +86-27-68754067.

[†] Wuhan University.

[‡] Stony Brook University.

[§] Chinese Academy of Sciences.

^{||} The University of Tokyo.

tion" of the self-assembled complex consisting of cellulose, NaOH, and urea hydrates. Our findings may lead to a new approach for the dissolution of a rather complex polymer, natural cellulose.

Experimental Section

Materials. Two samples (C-1 and C-2) of cellulose (the cotton linter pulp) were supplied by Hubei Chemical Fiber Co. Ltd. (Xiangfan, China). Their degrees of polymerization (DP) provided by the factory were ca. 620 for C-1 and 440 for C-2.⁸ Commercially available NaOH and urea were of guaranteed reagent levels (Shanghai Chemical Reagent Co. Ltd., China), and they were used without further purification. Urea-¹⁵N₂ with 98% ¹⁵N content (Aldrich) was used for ¹⁵N NMR measurement. 7 wt % NaOH–12 wt % urea aqueous solution as the solvent system for the C-2 cellulose sample was prepared by directly mixing of NaOH, urea, and distilled water with NaOH:urea:H₂O at a weight ratio of 7:12:81.

Preparation of Cellulose Solution. A known weight of cellulose was dispersed into 7 wt % NaOH–12 wt % urea aqueous solution precooled to –12 °C and then stirred for 5 min to obtain a transparent 4 wt % cellulose solution. To prepare dilute cellulose solution, 15 g of NaOH, 23 g of urea, and 162 mL of dilute water were mixed, and the resulting solution system was filtered by using a 0.22 μm filter. The solvent system was stored at 5 °C before use. The weighted cellulose was dispersed in the solvent, stirred for 5 min, and stored in a refrigerator to reach –12.5 °C. The cooled liquid was stirred extensively at ambient temperature (below 15 °C) to get a colorless transparent solution. The dilute cellulose solution was used to determine the cellulose molecular weight and for transmission electron microscopy. The original concentration of the cellulose solution was 5×10^{-4} – 10×10^{-4} g/mL.

Characterization. ¹³C NMR measurements of two cellulose (C-2) solutions in 7 wt % NaOH–12 wt % urea–D₂O and 9 wt % NaOH–D₂O were carried out on a Mercury 600 MHz NMR spectrometer (Varian, Inc.) at ambient temperature. The sodium salt of 2,2-dimethyl-2-silapentane-5-sulfonic acid (DSS) was used as an internal reference to determine the chemical shifts. ¹⁵N and ¹H NMR measurements of 7 wt % NaOH–12 wt % urea–D₂O and cellulose solutions in 7 wt % NaOH–12 wt % urea–D₂O were carried out on a JNM-A500 FT NMR system (JEOL, Japan) at ambient temperature. The ammonia liquid was used as reference for chemical shift of ¹⁵N. The cellulose concentration was adjusted to be 4 wt %. The Fourier transform infrared (FT-IR) spectrum was recorded with a Bruker Equinox 55S FT-IR spectrometer (Germany) equipped with a variable temperature cell (P/N 21525, SPECA Inc.). For each spectrum, 32 scans were recorded and averaged. The low-temperature measurements were performed with a laboratory-designed liquid nitrogen cooled cryostat, consisting of a copper sample holder with a small container that was filled with liquid nitrogen. It was surrounded by a jacket with KBr windows and placed under N₂ gas flow. The solvent system was sealed between two pieces of CaF₂ crystals for FTIR measurements. FTIR data were taken at temperatures from –40 to 15 °C.

Wide-angle X-ray diffraction (WAXD) experiments were carried out at the Advanced Polymers Beamline (X27C) in the National Synchrotron Light Source (NSLS), Brookhaven National Laboratory (BNL). The wavelength was 0.1371 nm. The sample was put in a stainless sample holder, and the temperature of the sample was controlled by a hot stage (Instec, Inc.). WAXD measurements at different temperatures were carried out for 7 wt % NaOH–9 wt % urea aqueous solutions. The frozen-dried sample was prepared from 4 wt % cellulose–7 wt % NaOH–9 wt % urea aqueous solution. Solid urea and NaOH were ground into powder before synchrotron X-ray measurements.

Transmission electron microscope (TEM) observation of the morphology of cellulose in NaOH–urea aqueous solution was carried out on a JEM-2010 (HT) transmission electron microscope (JEOL TEM, Japan). A thin layer of the dilute cellulose solution was suspended on a holey carbon film, which was supported on a

copper grid. The specimen was dried in air at ambient temperature within 10 min and then was imaged on TEM at an accelerating voltage of 200 kV. Two dilute solutions of the C-2 cellulose sample in NaOH–urea and NaOH aqueous solution at a concentration of 4.0×10^{-4} g/mL were used here for comparison purposes.

Small-angle neutron scattering (SANS) was one of the main tools used in our approach. The measurements were made at the National Institute of Standard and Technology Center for Neutron Research (NCNR). The angular dependence of excess scattering was measured in the range of 0.2°–24°. In SANS, the essential measurement length scale is the reciprocal of the scattering vector q , that is $1/q$, with

$$q = \frac{4\pi}{\lambda} \sin \frac{\theta}{2} \quad (1)$$

where λ is the neutron wavelength and θ is the scattering angle.²²

Static and dynamic light scatterings (SLS and DLS) were used to characterize the molecular weight and chain conformation of cellulose in the dilute solution (NaOH–urea aqueous system). A modified commercial light scattering spectrometer (ALV/SP-125, ALV, Germany) equipped with an ALV-5000/E multi- τ digital time correlator and a He–Ne laser (at $\lambda = 632.8$ nm) was used at scattering angle θ of 30°. All of the C-1 cellulose solutions were prepared at the concentration of 1.0×10^{-4} – 8.0×10^{-4} g/mL and made optically clean by filtration through 0.45 μm Millipore filters. A Zimm plot was used to calculate the weight-average molecular weight (M_w) and the radius of gyration ($\langle R_g \rangle$). The CONTIN program²³ was used for the analysis of dynamic light-scattering data. The hydrodynamic radius, R_h , was calculated by using the Stokes–Einstein relation as

$$R_h = \frac{k_B T}{6\pi\eta_0 D} \quad (2)$$

where k_B is the Boltzmann constant, T the temperature in units of K, η_0 the solvent viscosity, and D the translational diffusion coefficient.

Results and Discussion

Effect of Low Temperature. Figure 1 shows FT-IR spectra of H₂O (a), 7 wt % NaOH (b), 12 wt % urea (c), and 7 wt % NaOH–12 wt % urea (d) aqueous solutions at various temperatures. Infrared spectroscopy has been used to analyze the hydrogen-bonded network structure in water clusters, indicating that the envelopes associated with hydrogen bonds (3000–3600 cm^{−1}) blue shift with increasing cluster size.^{24–26} As shown in Figure 1, there was a broad band for all samples, and those of 7 wt % NaOH and 7 wt % NaOH–12 wt % urea aqueous solutions (b and d) were significantly blue-shifted, and their intensity increased with decreasing temperature from 13 to –40 °C. Moreover, a shoulder peak (3200–3400 cm^{−1}) appeared in the FT-IR spectra, which is relative to an increase of water clusters with a fully bonded network.²⁵ The blue-shifted peak (b to d) and increased intensity proved that the hydrogen-bonded networks structure and cluster size in NaOH and NaOH–urea aqueous systems increased gradually. Namely, the low temperature promoted the formation of the hydrogen-bonded network of NaOH, urea, and water molecules.

Figure 2 shows 1D WAXD intensity profile of the NaOH–urea solvent system at different temperatures. The intensity of a strong wide peak, centered at around scattering vector (s) = 3.2 nm^{-1} , was highest at about –10 °C. This indicated that the highest amount of the complex associated with urea and NaOH could occur in aqueous solution at this low temperature. A maximum value of this peak suggested that the complex formation could be thermodynamically more favorable at this low temperature while it was less favorable when the temperature was further increased. It is noted that this temperature is

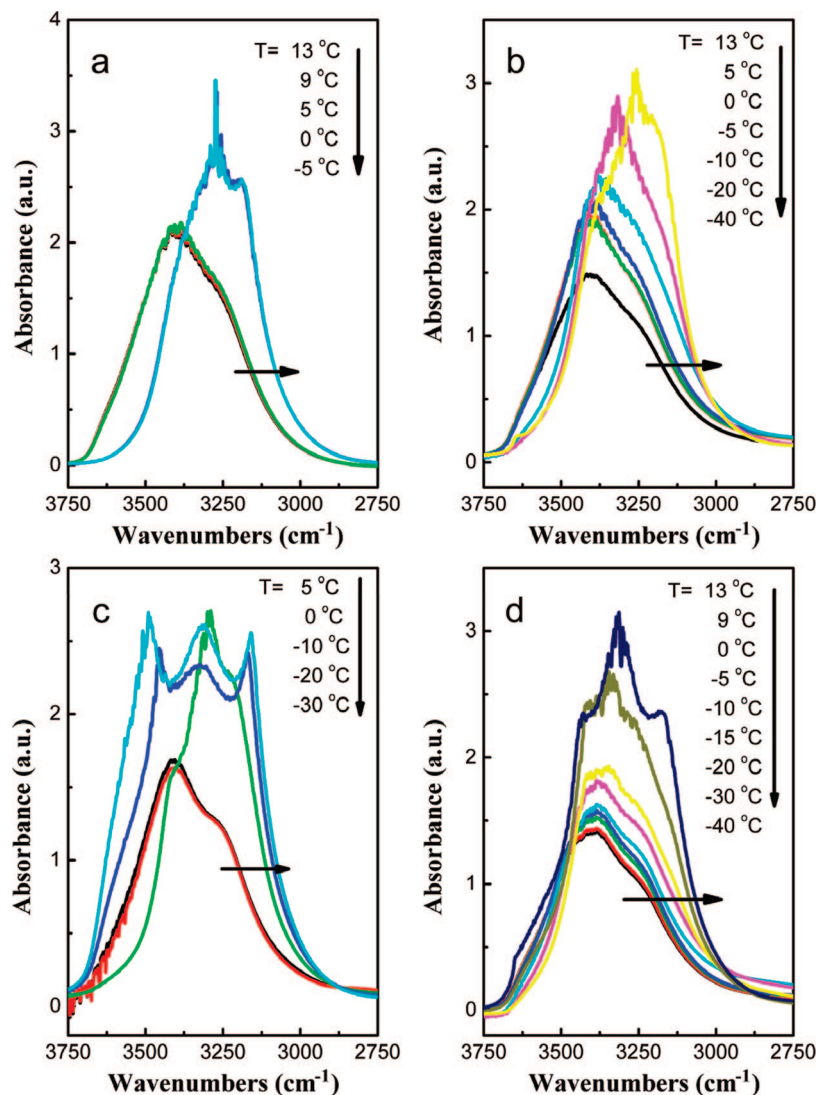


Figure 1. FTIR spectra of H₂O (a), 7 wt % NaOH (b), 12 wt % urea (c), and 7 wt % NaOH–12 wt % urea (d) aqueous solution at different temperature. The band having high intensity represents ice-like water, so others at more low temperature are not shown here.

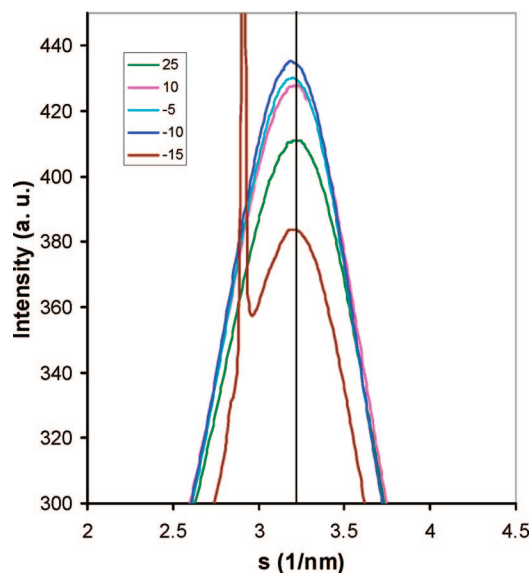


Figure 2. 1D WAXD intensity profile of 7 wt % NaOH–12 wt % urea aqueous solution at different temperatures (inset, °C).

close to the optimized dissolving temperature (−12 °C) for cellulose in 7 wt % NaOH–12 wt % urea aqueous solution. At

temperatures lower than −10 °C, the intensity of this peak was decreased possibly due to the crystallization effects in the aqueous solution at lower temperatures. The sharp new peak on the WAXS profile at −15 °C corresponded to one of strong reflections from the crystal formed in urea and NaOH aqueous solution, revealing that the solvent system would begin to crystallize if the temperature was decreased to −15 °C and, therefore, leading to a drop in the amount of the complex associated with urea and NaOH in the aqueous solution. Furthermore, the position of those broad peaks in Figure 2 shifted slightly to lower values with decreasing temperature, indicating that the dimensions of the complex could have increased. The results from WAXD further confirmed the supposition that the relatively stable complex associated with NaOH, urea, and water via the hydrogen-bonding networks could exist at low temperatures.

Figure 3 shows SANS profiles of solvents with different components at 0 °C. The SANS results proved that the NaOH–D₂O aqueous system was more uniform than that of the urea–D₂O aqueous system, leading to a slope at low q and suggesting an “infinitely” large clusters in the observation range of SANS. However, the mixture of NaOH and urea in D₂O formed clusters with smaller sizes based on the smaller slope values at low q , suggesting that the addition of NaOH weakened the association of urea in water. Porod exponents for urea–D₂O

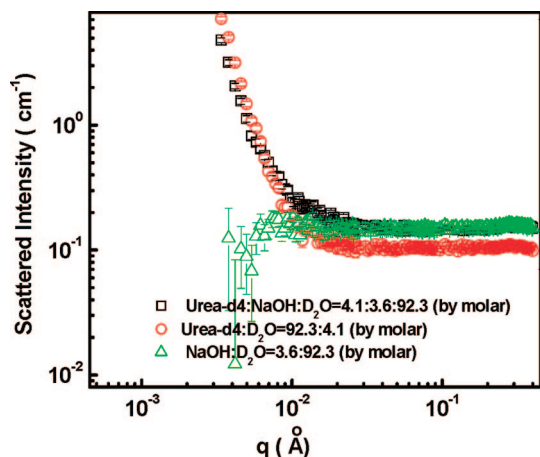


Figure 3. SANS profiles of solvents with different components at 0 °C.

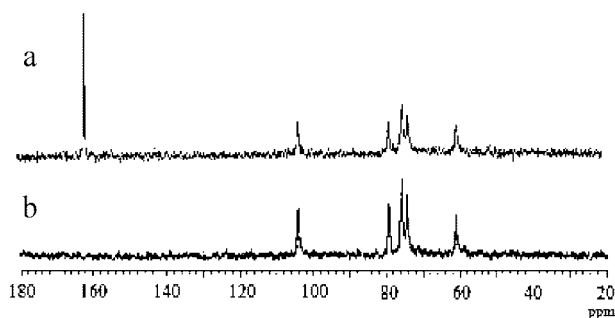


Figure 4. ^{13}C NMR spectra of cellulose (C-2) solution in 7 wt % NaOH-12 wt % urea- D_2O (a) and in 9 wt % NaOH- D_2O (b) at 18 °C.

and NaOH-urea- D_2O were 3.2 and 2.8, which could be related to the surface fractal and mass fractal, respectively. This meant that the cluster size in urea- D_2O without NaOH could be larger than that in NaOH-urea- D_2O , indicating a stronger interaction between NaOH and urea compared to urea and water. A/q^n over a sufficiently large q range can be used as a measure of clustering strength. Therefore, the clustering strength of the NaOH-urea was much higher than that of urea- D_2O . This can be explained by the cluster size²⁷ and the random network structure of urea and water.²⁸ In view of the results from FT-IR, WAXD, and SANS, the complex associated with urea and NaOH hydrates as the predominant species existed in the NaOH-urea- D_2O system, and the hydrogen-bonded network structure was at a highly stable state at low temperatures to create their supramolecular assembly.

Interactions between Cellulose and Solvent Components.

The rapid dissolution of cellulose in NaOH/urea aqueous solution indicated actually that the strong interaction between cellulose and solvent have occurred in the aqueous system to cleave the chains packing of cellulose through the formation of new hydrogen bonds at low temperatures. Figure 4 shows ^{13}C NMR spectra of the C-2 cellulose sample in 7 wt % NaOH-12 wt % urea- D_2O and 7 wt % NaOH- D_2O solutions, respectively. The chemical shift of the carbonyl carbon for urea in 7 wt % NaOH-12 wt % urea- D_2O solution is at 162.4 ppm. In addition, six major peaks for the cellulose solutions were readily identified, each exhibiting an apparent sharpness.^{5,6} The chemical shifts of C_1 (104.4 ppm), C_4 (79.6 ppm), $\text{C}_{3,5}$ (76.2 ppm), C_2 (74.5 ppm), and C_6 (61.2 ppm) for cellulose in 7 wt % NaOH-12 wt % urea- D_2O were similar to that in the 9 wt % NaOH- D_2O solution, indicating that the magnetic environment of cellulose molecules in the alkali-urea system is the same as

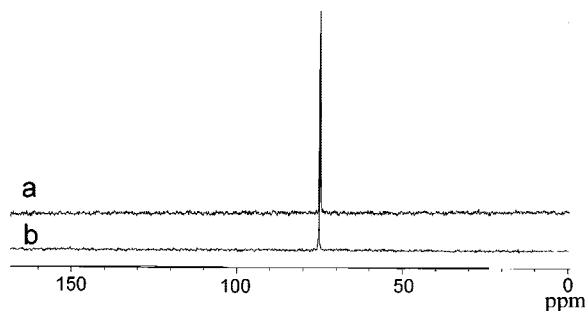


Figure 5. ^{15}N NMR of 7 wt % NaOH-12 wt % urea- D_2O solution (a) and 4 wt % cellulose-7 wt % NaOH-12 wt % urea- D_2O solution (b).

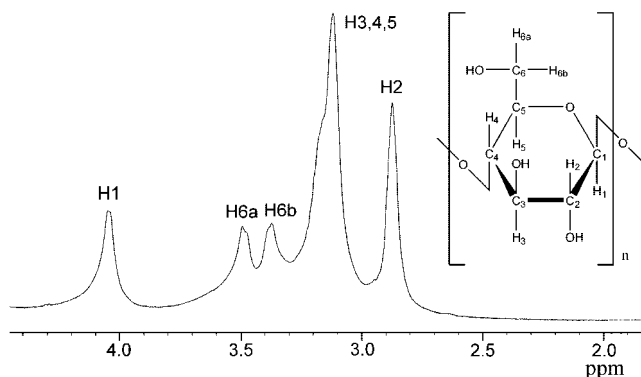


Figure 6. ^1H NMR of 4 wt % cellulose-7 wt % NaOH-12 wt % urea- D_2O solution.

in the alkali-only system. This situation has been further confirmed by the ^{15}N NMR spectra of 7 wt % NaOH-12 wt % urea- D_2O solvent and its cellulose solution using ^{15}N -urea (98% purity in ^{15}N). The ^{15}N peak of urea in the cellulose solution was identical with that in the solvent, without any splitting to suggest specific interactions (indirect) between urea and cellulose molecules. Furthermore, the ^1H NMR spectrum of the cellulose's C-H in 7 wt % NaOH-12 wt % urea- D_2O solution (Figure 6) was highly similar to that in NaOH-only system reported by Isogai.²⁹ The hydroxyl protons of the anhydroglucose residue are involved in the peak of HOD at around 4.7 ppm by deuteration with NaOH-urea- D_2O . Moreover, the overall extent of shift in C-H peak positions of cellulose in the 7 wt % NaOH-12 wt % urea- D_2O solution was corresponding to those in 20–24% NaOH reported by Isogai.²⁹ These results strongly support that cellulose chains have been surrounded directly by NaOH hydrates, and the urea hydrate molecules were present outside of this sheathlike structure of NaOH hydrate for cellulose.

Usually, the OH^- ions exist as $[\text{OH}(\text{H}_2\text{O})_n]^-$ and the Na^+ ion as $[\text{Na}(\text{H}_2\text{O})_m]^+$ in NaOH aqueous solution. At room temperature, the fast exchange between bulk water and coordinated water makes the $[\text{OH}(\text{H}_2\text{O})_n]^-$ and $[\text{Na}(\text{H}_2\text{O})_m]^+$ ions difficult to maintain a stable structure, whereas at low temperatures, the slower exchange enables the coordinated ion to keep its structure. Therefore, in the cellulose-NaOH-urea aqueous system at -12 °C, being very close to the melting point of the solvent system, the $[\text{OH}(\text{H}_2\text{O})_n]^-$ ions could be more easily attracted to the cellulose chains, leading to the breakdown of intra- and intermolecular hydrogen bonds among the cellulose. However, the cellulose solution in the NaOH aqueous system without urea was less stable, leading to lower solubility. We did not obtain the ^{13}C NMR spectra of cellulose in the urea aqueous system because cellulose could not be dissolved, indicating that urea was unable to associate directly with

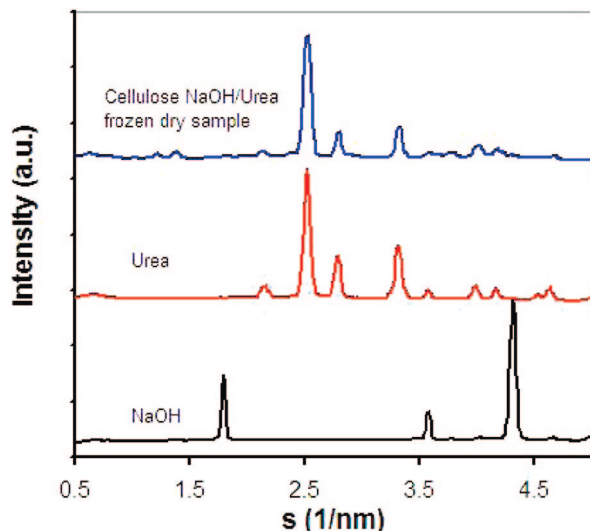


Figure 7. 1D WAXD intensity profile of NaOH (powder), urea (powder), and cellulose in NaOH–urea solution and then frozen and dried.

cellulose. It has been reported that urea can form easily inclusion compounds^{30,31} and could encaged guest molecules with urea molecules at the surface of the layers. Our findings have confirmed that NaOH “hydrates” in the NaOH–urea cluster could be more easily attracted to the cellulose chain through the formation of new more stable hydrogen-bonded networks at low temperatures. Moreover, urea could associate easily with NaOH hydrate to surround. Thus, we proposed that urea hydrates would be self-assembled at the surface of the cellulose hydrogen-bonded with NaOH hydrates to form an inclusion complex (IC).

Inclusion Complex Surrounded by Urea. Figure 7 shows WAXD intensity profile of pure NaOH, urea, and freeze-dried sample from cellulose (C-1) in 7 wt % NaOH–12 wt % urea aqueous solution. The major peaks at s values of 2.56, 2.84, and 3.36 nm^{−1} were assigned to the tetragonal crystal of urea. Interestingly, the WAXD intensity profile of the cellulose in NaOH–urea solution was similar to that of pure urea (powder), and the peaks of NaOH and cellulose disappeared in this profile. This indicated that complex formed from cellulose and NaOH hydrates was engaged in the urea host, leading to the shield for cellulose and NaOH. Therefore, the urea hydrates have aggregated at the surface of the new hydrogen-bonded networks associated with cellulose and NaOH to create the cellulose IC surrounded by urea.

To provide additional direct evidence on the cellulose ICs in NaOH–urea aqueous solution, transmission electron microscopy was used to observe their morphology. The TEM images of the cellulose dilute solution *dried* at room temperature are shown in Figure 8. As expected, the images displayed a wormlike pattern, which was the cellulose IC rather than NaOH or urea (Supporting Information, Figure S1), and their surface was surrounded by the partial melting of urea as shown in Figure 8a–c. It presents a kebab shape rather than a homogeneous surface because the electron beam struck the nonmetal sample, resulting in the partial melting of urea on the surface of the cellulose IC. With an increase in the TEM measurement time from 1 to 20 min, the morphology of the wormlike ICs changed from the shish-kebab shape to a flat strip as shown in Figure 8b. Moreover, there was no electronic diffraction pattern of the crystallization structure on the surface of the cellulose IC obtained from the cellulose solution in the NaOH–urea system (inset in Figure 8a). Interestingly, there was only thin film of self-aggregated cellulose chains in the NaOH aqueous solution without urea (Figure 8d). The electron diffraction (ED) pattern

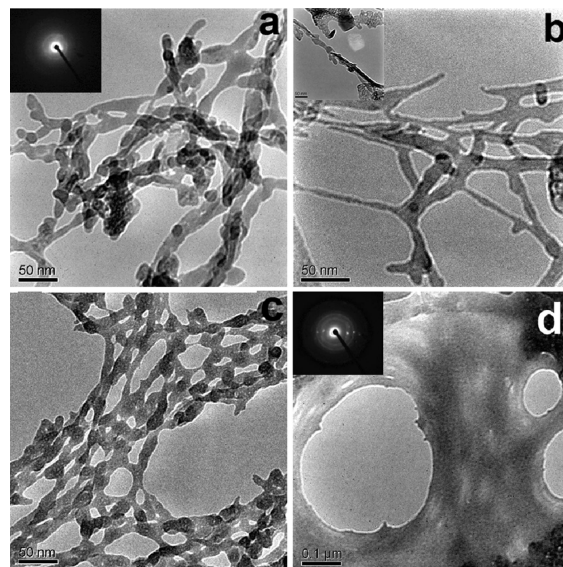


Figure 8. TEM images of cellulose solution at 5.0×10^{-4} g/mL in 7 wt % NaOH–12 wt % urea aqueous solution (a and b); the TEM observation within 2 min for (a) and after 20 min for (b); TEM images of cellulose solution after storing for 12 h at 5 °C (c); cellulose solution at 5.0×10^{-4} g/mL in 7 wt % NaOH aqueous solution without urea (d). The insets (a, d) present their electron diffraction (ED) pattern of the surface, and (b) shows melting urea on the surface of the cellulose IC.

of the surface for the cellulose–NaOH complex (inset of Figure 8d) indicated the crystallization structure of cellulose and NaOH. It further confirmed that the surface of the cellulose bonded with NaOH hydrates were surrounded by urea hydrates. The individual cellulose molecules encaged with urea and NaOH hydrates could be linked with each other, forming longer, parallel, and overcross aggregates as a result of the part dissociation of IC. A similar phenomenon has been observed for cellulose in the LiOH–urea aqueous solvent system by TEM and WAXD, indicating that urea hydrates could encage the cellulose macromolecules hydrogen-bonded with LiOH.³⁰ It was suggested that the self-assembly was unstable system, namely the existence of dynamical fluctuations.

Dynamic Self-Assembly among Cellulose and Solvent. It is worth noting that cellulose could be dissolved in the NaOH–urea aqueous solution within 2 min on a typical laboratory scale and within 5 min even in a dissolution tank of 1000 L capacity (Jiangsu Long-Ma Green Fibers Co. Ltd.). In fact, perhaps only several seconds may be required because of the appearance of the Weissenberg phenomenon, that is, the polymer concentrated solution can wrap up a stirring shaft, within a 30 s time period. This interesting process, to our knowledge, represents the most rapid dissolution of native cellulose, not to mention the speed of the dissolution process. The interesting phenomenon of *rapid* dissolution of native cellulose actually suggests a dynamic self-assembly behavior. With NaOH and urea being aggregated on the cellulose chain as likely to be driven by hydrogen bonds, such structures are relatively unstable. Usually, dynamic self-assembly behavior is often a quick process. In our case, the hydrogen-bond-induced NaOH and urea to aggregate on cellulose into a specific structure, leading to the self-assembled IC. Interestingly, in our finding cellulose with dimensions of centimeters could be dispersed rapidly in the aqueous solution due to the aggregation of the solvent small molecules on the cellulose macromolecules, different from the self-assemble between macromolecules.

The LLS and DLS measurements have been used to investigate the self-assembly process as well as the shape and

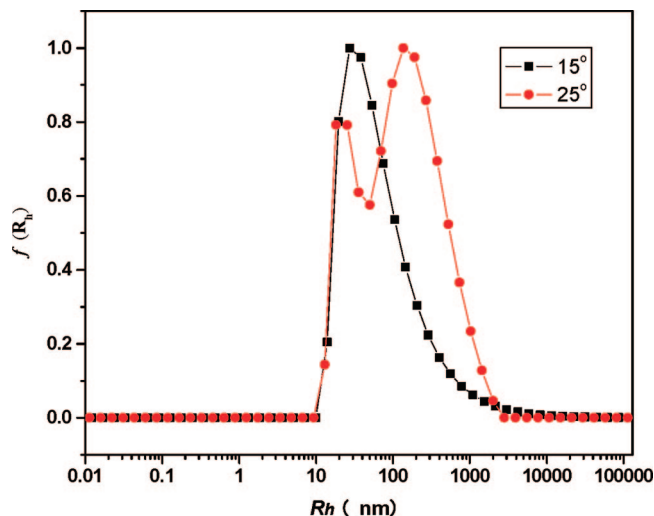


Figure 9. Hydrodynamic radius distributions $f(R_h)$ of the cellulose (C-1) solution in 7 wt % NaOH–12 wt % urea system with concentration of 1×10^{-4} g/mL at different temperatures (●, 15 °C; ▲, 25 °C) and scattering angle of 30°.

dimensions of the cellulose IC. It is difficult to truly disperse cellulose molecules in most “known” solvents at the molecular level, and the aggregation of cellulose in various solutions has been reported.⁷ Therefore, to reduce the gel formation, M_w , R_g , and R_h of the dilute cellulose (C-1) solution in the NaOH–urea system were measured within 2 h after preparation of the cellulose solution. The values of M_w and R_g of the cellulose (C-1) sample in the 7 wt % NaOH–12 wt % urea aqueous system at 15 °C were obtained from a Zimm plot (Supporting Information, Figure S2). The apparent weight-average molecular weights ($\langle M_{w,app} \rangle$) of the C-1 cellulose were obtained to be $\sim 1.1 \times 10^5$ and $2.0\text{--}4.0 \times 10^5$ g/mol at 15 and 25 °C, respectively, from numerous LLS measurements. It is noted that the dilute solution exhibited less aggregates at 15 °C; namely, a substantial amount of cellulose chains in the NaOH–urea system could exist as single chains, whereas it formed relatively more and larger size aggregates at 25 °C. The apparent average radius of gyration ($\langle R_{g,app} \rangle$) of cellulose in the NaOH–urea aqueous system was calculated to be 60–75 nm in the presence of a reasonable amount of single chains. The difference in the $\langle M_{w,app} \rangle$ and $\langle R_{g,app} \rangle$ values implied that the cellulose solution in this solvent system was not stable. Furthermore, the particle size and shape of the cellulose IC could change with temperature changes as a result of the part dissociation of IC in the system.

The hydrodynamic radius distributions $f(R_h)$ of the cellulose (C-1) solution in 7 wt % NaOH–12 wt % urea system at different temperatures and at different storage time are shown in Figures 9 and 10. The CONTIN analysis of DLS measurements on the cellulose solution was performed. The peak with lower hydrodynamic radii ($\langle R_h \rangle$) could represent individual cellulose chains, whereas that with a higher $\langle R_h \rangle$ value could be attributed to its aggregates. The apparent average $\langle R_h \rangle_{app}$ obtained from the cumulative analyses were ~ 25 nm for the single chains and ~ 160 nm for aggregates in the cellulose solution with different concentration from 1.0×10^{-4} to 10×10^{-4} g/mL at 15 and 25 °C. The macromolecular shape can be judged from the value of R_g/R_h , which directly reflects the chain conformation. For a flexible chain in a good solvent the mean value of R_g/R_h lies in the range from 1.5 to 1.8; for an extended chain (wormlike or rodlike chain), R_g/R_h is more than 2.0.^{32,33} By using the $\langle R_{g,app} \rangle$ and $\langle R_{h,app} \rangle$ values for the single chains as predominant species, the apparent average ratio of $\langle R_g/R_h \rangle_{app}$ has been estimated to be ~ 2.5 , indicating an extended chain in the dilute solution. The results of SLS and DLS indicated that

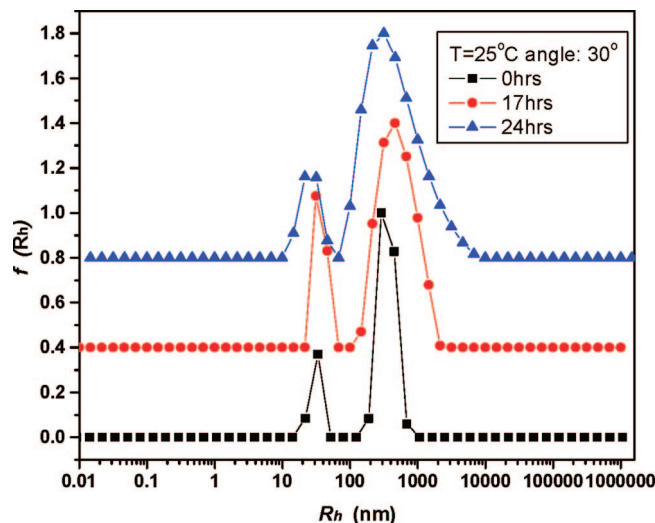


Figure 10. DLS profiles of the cellulose (C-1) solution with concentration of 4.7×10^{-4} g/mL in NaOH–urea solvent at different storage time (■, 0 h; ●, 17 h; ▲, 24 h) and scattering angle of 30°.

most cellulose molecules, with limited amounts of aggregation, could exist as extended rigid chains in dilute solution. This was supported by the IC patterns in TEM. The extended cellulose chains could be of benefits to the orientation of regenerated cellulose fibers, leading to good mechanical properties.³⁴ Further, with the prolonging of the stored time (Figure 10) or with an increase of polymer concentration (Supporting Information, Figure S3), the peaks corresponding to aggregates shifted to higher R_h on the whole, indicating an enhancement of the cellulose aggregation. In view of the results from scattering experiments, the cellulose solution was relatively unstable and could be very sensitive to temperature, polymer concentration, and storage time, leading to additional aggregations. These results have indicated that the ICs exhibited a dynamic structure which can be affected by temperature, polymer concentration, and storage time.

From the analysis of our findings, the dynamic self-assembly process in the cellulose–NaOH–urea aqueous system at -12 °C could be described as follows. When the cellulose solid was immersed in the precooled solvent, a new hydrogen-bonded network structure between the cellulose macromolecules and solvent small molecules was created rapidly to form a wormlike cellulose IC being surrounded with urea. The self-assembled IC brought cellulose into a complex formation which became soluble in the aqueous solution system. The urea hydrates located on the outside of the cellulose ICs reduced greatly the entanglement and self-association of the cellulose molecules in the solution system, leading to the increased solubility and stability.

Conclusion

The rapidly dissolution of cellulose in precooled (-12 °C) 7 wt % NaOH–12 wt % urea aqueous solution could be associated with the formation of new hydrogen-bonded network structure in the system, which was at a highly stable state at low temperatures. The NaOH “hydrates” could be more easily attracted to cellulose chains through the formation of new hydrogen-bonded networks at low temperatures, while the urea hydrates could not be associated directly with cellulose. The experimental results revealed that the cellulose dissolution arose as a result of a dynamic self-assembly process among solvent molecules (NaOH, urea, and water) and cellulose macromolecules. A wormlike IC engaging the cellulose chain could be self-assembled rapidly from NaOH–urea–water clusters and

cellulose through the formation of new hydrogen-bonding networks at low temperatures, leading toward a quick “dissolution” of cellulose. The cellulose solution could be very sensitive to temperature, polymer concentration, and storage time, leading to a dynamic structure in the system. The self-assembled clusters created a possible new pathway for the “dissolution” of natural polymers through the hydrogen-bonded arrangement of macromolecules and some special small molecules in an aqueous system.

Acknowledgment. This work was supported by High-Technology Research and Development Program of China (2003AA333040), major grant of the National Natural Science Foundation of China (59933070 and 30530850), the National Natural Science Foundation of China (20874079), the US National Science Foundation and the US Department of Energy. J.C. thanks Dr. Hiroe Narita for helpful discussions and NMR characterization assistance.

Supporting Information Available: TEM images of 7 wt % NaOH aqueous solution and 7 wt % NaOH–12 wt % urea aqueous solution (Figure S1); Zimm plot for the cellulose (C-1) dilute solution in 7 wt % NaOH–12wt % urea aqueous system at 15 °C (Figure S2); DLS profiles of cellulose solution with different concentration (C-1) in NaOH/urea solvent (Figure S3). This material is available free of charge via the Internet at <http://pubs.acs.org>.

References and Notes

- (1) Klemm, D.; Heublein, B.; Fink, H. P.; Bohn, A. *Angew. Chem., Int. Ed.* **2005**, *44*, 3358–3393.
- (2) Johnson, D. L. *Brit.* 1144048, **1967**.
- (3) Fink, H. P.; Weigel, P.; Purz, H. J.; Ganster, J. *Prog. Polym. Sci.* **2001**, *26*, 1473–1524.
- (4) Swatloski, R. P.; Spear, S. K.; Holbrey, J. D.; Rogers, R. D. *J. Am. Chem. Soc.* **2002**, *124*, 4974–4975.
- (5) Cai, J.; Zhang, L. *Macromol. Biosci.* **2005**, *5*, 539–548.
- (6) Cai, J.; Zhang, L. *Biomacromolecules* **2006**, *7*, 183–189.
- (7) Chen, X.; Burger, C.; Wan, F.; Zhang, J.; Rong, L.; Hsiao, B.; Chu, B.; Cai, J.; Zhang, L. *Biomacromolecules* **2007**, *8*, 1918–1926.
- (8) Cai, J.; Zhang, L.; Zhou, J.; Qi, H.; Chen, H.; Kondo, T.; Chen, X.; Chu, B. *Adv. Mater.* **2007**, *19*, 821–825.
- (9) Liu, S.; Zhang, L.; Zhou, J.; Wu, R. *J. Phys. Chem. C* **2008**, *112*, 4538–4544.
- (10) Liu, S.; Zhang, L.; Zhou, J.; Xiang, J.; Sun, J.; Guan, J. *Chem. Mater.* **2008**, *20*, 3623–3628.
- (11) Song, Y.; Sun, Y.; Zhang, X.; Zhou, J.; Zhang, L. *Biomacromolecules* **2008**, *9*, 2259–2264.
- (12) Brubach, J. B.; Mermet, A.; Filabozzi, A.; Gerschel, A.; Roy, P. *J. Chem. Phys.* **2005**, *122*, 184509.
- (13) Whitesides, G. M.; Grzybowski, B. *Science* **2002**, *295*, 2418–2421.
- (14) Yan, D.; Zhou, Y.; Hou, J. *Science* **2004**, *303*, 65–67.
- (15) Zhou, Y.; Yan, D. *Angew. Chem., Int. Ed.* **2004**, *43*, 4896–4899.
- (16) Li, S.; He, P.; Dong, J.; Guo, Z.; Dai, L. M. *J. Am. Chem. Soc.* **2005**, *127*, 14–15.
- (17) Jones, M. C.; Tewari, P.; Blei, C.; Hales, K.; Pochan, D. J.; Leroux, J. C. *J. Am. Chem. Soc.* **2006**, *128*, 14599–14605.
- (18) Liu, S.; Hu, T.; Liang, H.; Jiang, M.; Wu, C. *Macromolecules* **2000**, *33*, 8640–8643.
- (19) Fialkowski, M.; Bishop, K. J. M.; Klajn, R.; Smoukov, S. K.; Campbell, C. J.; Grzybowski, B. A. *J. Phys. Chem. B* **2006**, *110*, 2482–2496.
- (20) Groot, S. R. D.; Mazur, P. *Nonequilibrium Thermodynamics*; Dover Publications: New York, 1984.
- (21) Tsunashima, Y.; Kawanishi, H.; Horii, F. M. *Biomacromolecules* **2002**, *3*, 1276–1285.
- (22) Higgins, J. S.; Benoit, H. C. *Polymers and Neutron Scattering*; Clarendon Press: Oxford, 1994.
- (23) Chu, B. *Laser Light Scattering*, 2nd ed.; Academic Press: New York, 1991.
- (24) Asbury, J. B.; Steinel, T.; Fayer, M. D. *J. Phys. Chem. B* **2004**, *108*, 6544–6554.
- (25) Miyazaki, M.; Fujii, A.; Ebata, T.; Mikami, N. *Science* **2004**, *304*, 1134–1137.
- (26) Shin, J. W.; Hammer, N. I.; Diken, E. G.; Johnson, M. A.; Walters, R. S.; Jaeger, T. D.; Duncan, M. A.; Christie, R. A.; Jordan, K. D. *Science* **2004**, *304*, 1137–1140.
- (27) Hammouda, B.; Ho, D. L.; Kline, S. *Macromolecules* **2004**, *37*, 6932–6937.
- (28) Vanzi, F.; Madan, B.; Sharp, K. *J. Am. Chem. Soc.* **1998**, *120*, 10748–10753.
- (29) Isogai, A. *Cellulose* **1997**, *4*, 99–107.
- (30) Cai, J.; Zhang, L.; Chang, C.; Cheng, G.; Chen, X.; Chu, B. *ChemPhysChem* **2007**, *8*, 1572–1579.
- (31) Lee, S. O.; Kariuki, B. M.; Harris, K. D. M. *Angew. Chem., Int. Ed.* **2002**, *41*, 2181–2184.
- (32) Niu, A.; Liaw, D.; Sang, H.; Wu, C. *Macromolecules* **2000**, *33*, 3492–3494.
- (33) Nie, T.; Zhao, Y.; Xie, Z.; Wu, C. *Macromolecules* **2003**, *36*, 8825–8829.
- (34) Kong, K.; Davies, R. J.; McDonald, M. A.; Young, R. J.; Wilding, M. A.; Ibbett, R. N.; Eichhorn, S. J. *Biomacromolecules* **2007**, *8*, 624–630.

MA801110G